



Published in final edited form as:

Biomaterials. 2008 June ; 29(18): 2705–2709.

The role of cerium redox state in the SOD mimetic activity of nanoceria

Eric Heckert¹, Ajay Karakoti², Sudipta Seal^{2,3}, and William T. Self^{1,*}

¹ Department of Molecular Biology and Microbiology, Burnett School of Biomedical Science, College of Medicine, 4000 Central Florida Blvd., Bldg. 20 Room 124, University of Central Florida, Orlando, Florida 32816-2364, Telephone (407) 823-4262, Fax (407) 823-0956

² Advanced Materials Processing and Analysis Center, Mechanical Materials Aerospace Engineering

³ Nanoscience Technology Center (NSTC), University of Central Florida, Orlando, Florida 32816

Abstract

Cerium oxide nanoparticles (nanoceria) have recently been shown to protect cells against oxidative stress in both cell culture and animal models. Nanoceria has been shown to exhibit superoxide dismutase (SOD) activity using a ferricytochrome C assay, and it is this mimetic activity that has been postulated to be responsible for cellular protection by nanoceria. The nature of nanoceria's antioxidant properties, specifically what physical characteristics make nanoceria effective at scavenging superoxide anion, is poorly understood. In this study electron paramagnetic resonance (EPR) analysis confirms the reactivity of nanoceria as an SOD mimetic. X-ray photoelectron spectroscopy (XPS) and UV-visible analysis of nanoceria treated with hydrogen peroxide demonstrate that a decrease in the Ce 3⁺/4⁺ ratio correlates directly with a loss of SOD mimetic activity. These results strongly suggest that the surface oxidation state of nanoceria plays an integral role in the SOD mimetic activity of nanoceria and that ability of nanoceria to scavenge superoxide is directly related to cerium (III) concentrations at the surface of the particle.

1.0 Introduction

Cerium is a lanthanide series rare earth element, and is the most abundant of these rare earths, present at about 66 parts per million in the earth's crust. Cerium can exist in either the free metal or oxide form, and can cycle between the cerous, cerium (III), and ceric, cerium (IV), oxidation states [1]. Both oxidation states of cerium strongly absorb ultraviolet light and have two characteristic spectrophotometric absorbance peaks. The first peak is in the 230 to 260 nm range and corresponds to cerium (III) absorbance. The second peak absorbance occurs in the 300 to 400 nm range and corresponds to cerium (IV) absorbance [2].

Nanoceria has similar chemical and physical properties to bulk cerium, however, because of the increased surface area and oxygen vacancies present, nanoceria has potential as a unique catalyst [3]. Much of the unusual catalytic chemistry involved with nanoceria is believed to be due to oxygen vacancy sites at the surface of the nanoceria lattice. These oxygen vacancies are characterized by cerium (III) atoms in the center of the vacancy surrounded by adjacent cerium (IV) atoms [4]. The presence of cerium (III) at the surface of nanoceria is unique to the center

* To whom correspondence is requested, W. T. Self wself@mail.ucf.edu; fax (407) 823-0956.

Publisher's Disclaimer: This is a PDF file of an unedited manuscript that has been accepted for publication. As a service to our customers we are providing this early version of the manuscript. The manuscript will undergo copyediting, typesetting, and review of the resulting proof before it is published in its final citable form. Please note that during the production process errors may be discovered which could affect the content, and all legal disclaimers that apply to the journal pertain.

of the oxygen vacancy and the relatively high abundance of these vacancies in nanoceria is speculated to be responsible for the altered redox chemistry of nanoceria versus bulk cerium [5].

Current research using nanoceria as a catalyst is quite broad. Among other applications, nanoceria is being developed for use in catalytic converters, as a scaffolding for carbonic anhydrase inhibitors, and as an oxygen sensor [6–9]. Oxidative stress generated from various endogenous sources has long been associated with cellular senescence and degenerative disease [10]. Because of the unique redox properties of cerium oxide and other lanthanide based metals, nanoceria is also being tested in both animal and cell culture models to determine its ability to protect against oxidative stress [7,11–13]. Specifically, glutamate induced excitotoxicity was reduced in HT22 neuronal cell model after treatment with cerium or yttrium nanoparticles [12]. Treatment of adult rat neurons with 10 nM nanoceria resulted in a decrease in cellular senescence after 30 days [14]. Transgenic mice expressing high levels of the chemoattractant MCP-1 were given nanoceria and showed reduced inflammation and cell death in a cardiovascular disease model [11]. These animal and cell culture studies demonstrate the effectiveness of nanoceria as an apparent antioxidant. However, the mechanism behind this protection is poorly understood and remains a gap in our knowledge today.

Prior literature suggests that the protective effects of nanoceria are a result of general radical scavenging capabilities. Currently, the only specific radical scavenging activity that has been reported is the SOD mimetic activity of nanoceria [7]. In this study, we further explore the mechanism behind this SOD mimetic activity, as it relates to the Ce $3^{+}/4^{+}$ ratio at the particle surface.

2.0 Materials and Methods

2.1 Materials

Xanthine oxidase and catalase were obtained from Sigma-Aldrich (St. Louis Missouri). Hydrogen peroxide and cytochrome C were from Acros Organics (Geel, Belgium). Tris was obtained from MP Biomedicals (Solon, Ohio). The radical spin trap 5-(Diethoxyphosphoryl)-5-methyl-1-pyrroline-N-oxide (DEPMPO) was from Axxora, LLC (San Diego, California). Nanoceria preparations were prepared as previously described [7]. Concentrations are reported as particles and based on average size of water-based synthesis preparations as described [7].

2.2 Spin-trap EPR studies

EPR was used to identify oxygen radicals using the spin trap DEPMPO as previously described [15]. Reactions were buffered using 100 μ M Tris buffer at pH 7.0. 30 mM DEPMPO and 50 μ M DPTA was added to all reactions. EPR spectra were acquired using a Bruker Elexsys E580 EPR spectrometer. All spectra were collected in perpendicular mode using a Bruker model ER 4122SHQE super-high Q resonator. EPR settings used to detect DEPMPO spin-trap adducts were: 20 mW microwave power, 20.48 ms time constant, 81.92 conversion time, 1.0 G modulation amplitude, field set = 3514, sweep with = 100 G, number of scans = 4.

2.3 UV-visible spectroscopy

UV-visible spectroscopy was used to measure the change in the oxidation state of nanoceria, in the presence or absence of the oxidizing agent hydrogen peroxide. Spectra for nanoceria were acquired using an Agilent 8453 UV-visible spectrophotometer (Santa Clara, CA) at room temperature in a 40 μ L microcuvette (Starna Cells, Atascadero, CA). An aliquot of nanoceria pretreated with 1.0 M H₂O₂, 0.1 M H₂O₂, or untreated ceria was diluted in water to a final

concentration of 750 nM (particle concentration). The UV-visible spectrum of nanoceria was recorded over a period of 16 days. Cuvettes were sealed to eliminate evaporation of the sample.

2.4 XPS analysis

XPS was performed using a 5400 PHI ESCA (XPS) spectrophotometer. The base pressure during the analysis was 10^{-9} torr and operated at a power of 300W using Mg K X-radiation. For XPS analysis, nanoceria samples were treated with 1.25 M hydrogen peroxide for 24 hours. Samples were then heated to remove excess water and peroxide and nanoceria was subsequently assayed for oxidation state. The samples were mounted on a carbon tape for XPS analysis. The charging shift was calibrated with the binding energy of Carbon (1s) as a baseline (284.6 eV).

2.5 Determination of hydrogen peroxide concentration

Hydrogen peroxide levels were detected using a 10-acetyl-3,7-dihydroxyphenoxazine (Amplex red) peroxidase assay kit from molecular probes (Eugene, OR). Amplex red has an excitation peak of 571 nm and an emission peak of 585 nm when converted to a fluorescent resorufin compound in the presence of horseradish peroxidase and hydrogen peroxide. Samples taken from the nanoceria incubation were diluted to reduce the target level of hydrogen peroxide to less than 5 μ M such that it is within the linear range of the enzyme-based assay. Fluorescence was measured in 96 well white microplates using a Varian Cary Eclipse spectrofluorometer (Varian, Palo Alto, CA) equipped with microplate reader. An excitation wavelength of 530 nm and an emission wavelength of 590 nm were used with slit widths of 5 nm and detection voltage at 400 V. A standard curve was generated using hydrogen peroxide. Peroxide levels are reported as the level remaining with respect to starting concentration (1.0 M or 0.1 M H_2O_2).

2.6 SOD mimetic assay

Reduction of ferricytochrome C was used to measure the SOD mimetic activity of nanoceria. Superoxide was generated by incubating 5 mM hypoxanthine and xanthine oxidase as previously described [7]. Xanthine oxidase concentration was adjusted prior to each experiment to insure that control samples reduced ferricytochrome C at a rate of 0.025 absorbance units per minute. Each assay was run at room temperature for five minutes in a 96 well plate with a total volume of 100 μ L. All reactions were buffered using 50 mM Tris buffer pH 7.5. The rate of ferricytochrome C reduction was measured by following an increase in absorbance at 550 nm using a Spectramax 190 UV-visible spectrophotometer (Molecular Devices, Sunnyvale, CA). Nanoceria samples were diluted to give 60 nM (particle) in the assay, as previously described [7]. During each time point control samples (no nanoceria) and 60 nM untreated nanoceria samples were run in parallel. All samples included 2,000 units of catalase to eliminate any residual hydrogen peroxide that may react either with nanoceria or ferricytochrome C.

3. 0 Results and discussion

3.1 EPR analysis

In order to corroborate the previously reported SOD mimetic activity of nanoceria that was based on ferricytochrome C assay, EPR was performed using hypoxanthine and xanthine oxidase to generate superoxide. Superoxide generated was measured using the spin trap DEPMPO as previously described [15,16]. In the presence of 750 nM nanoceria, the EPR signal intensity of a superoxide adduct of DEPMPO is significantly reduced (Figure 1). This intensity of a hydroxyl radical adduct, presumably produced by reaction of hydrogen peroxide and released iron, did not decrease in the presence of nanoceria (Figure 1). This confirms that

nanoceria catalyzes SOD activity and suggests that nanoceria may have some specificity for superoxide radicals. This argues directly against a general radical scavenging activity by this type of cerium oxide nanoparticle.

3.2 Oxidation of nanoceria by hydrogen peroxide

Having firmly established evidence that nanoceria can scavenge superoxide, by two different independent methods, further investigation is warranted to determine what physical properties play a role in its SOD mimetic activity. Previous studies have shown that hydrogen peroxide can oxidize the surface oxygen vacancies of nanoceria from cerium (III) to cerium (IV) [14]. If surface oxidation state is a key component of nanoceria SOD activity, then hydrogen peroxide would be an effective means to probe this possibility. Therefore, nanoceria was treated with 1.0 M or 100 mM hydrogen peroxide to alter the oxidation state of surface oxygen vacancies. Oxidation of nanoceria, specifically lowering the ratio of $Ce^{3+/4+}$, was confirmed using XPS analysis and clearly shows an increase in cerium (IV) present after treatment with hydrogen peroxide (Figure 2). A relative decrease in the intensity of peaks at 885.0 and 903.5 eV corresponding to the Cerium (III) oxidation state can be observed after the addition of hydrogen peroxide with a simultaneous rise in the relative intensity of peaks at 882.1, 898.0, 900.9, 906.4 and 916.4 eV corresponding to the cerium (IV). The treatment of nanoceria by hydrogen peroxide oxidized the surface of the nanoceria from (III) to (IV) as shown by the XPS spectra.

To measure changes in the oxidation state of nanoceria over time, UV-visible spectrophotometric analysis was performed. Oxidation of nanoceria by hydrogen peroxide should increase cerium (IV) concentrations and therefore should result in an increase in absorbance in the 300 to 400 nm range [2]. The 230 to 260 nm spectral range, which corresponds to the cerium (III) concentration, should also show a corresponding decrease in absorbance after the addition of hydrogen peroxide. Unfortunately, hydrogen peroxide absorbs strongly in this region. This makes following any spectrophotometric changes in cerium (III) concentration difficult (Figure 3A).

However cerium (IV) absorbance, which is not obscured by hydrogen peroxide, can still be used as a reliable and convenient method for measuring the surface oxidation state of nanoceria. UV-visible data shows a peak increase in absorbance in the 300 to 400 nm range approximately 48 hours after the addition of 1.0 M hydrogen peroxide (Figure 3B). This observed increase in absorbance is congruent with both previous literature and our own XPS data (Figure 2), and demonstrates that peroxides are capable of oxidizing nanoceria [17].

3.3 SOD mimetic activity of oxidized nanoceria

In order to assess the impact of oxidation state on SOD mimetic activity, nanoceria was tested using a ferricytochrome C assay during oxidation by hydrogen peroxide. Experiments were performed at various time points after the addition of hydrogen peroxide and were conducted over a period of approximately two weeks. Hydrogen peroxide treated nanoceria lost nearly all detectable SOD mimetic activity within 48 hours (Figure 4). Over the following 14 days, peroxide-treated nanoceria regained nearly 100% of the original mimetic activity when compared to untreated samples (Figure 4). This clearly shows that hydrogen peroxide is capable of temporarily inactivating the SOD mimetic activity of nanoceria. However, the observed inactivation is only transient; that is as hydrogen peroxide decomposes, nanoceria regains SOD mimetic activity. Comparing of the reduction state of nanoceria (Figure 3) to the SOD mimetic activity (Figure 5) it is clear that the changes in spectrophotometric absorbance over time matched inhibition in SOD mimetic activity. The return of SOD mimetic activity was accompanied by a corresponding drop in absorbance at 300–400 nm. This strongly suggests that the cerium (III) to cerium (IV) ratio is directly related to the reported SOD mimetic activity.

This data also agrees with XPS analysis that showed nanoceria preparations containing high amounts of cerium (IV) were ineffective in SOD mimetic assays [7].

Hydrogen peroxide levels in treated nanoceria were also measured in parallel (Figure 6). The results clearly show a reduction in peroxide concentration over time, however when compared to SOD mimetic assays (Figure 4), there appears to be little correlation between absolute peroxide levels and the SOD mimetic activity of nanoceria. This information suggests that the oxidation of nanoceria from cerium (III) to cerium (IV) is responsible for the resultant loss in SOD mimetic activity and is not related to residual peroxide. Altogether, this data suggests that the only relevant effect of hydrogen peroxide on nanoceria is to oxidize nanoceria from cerium (III) to cerium (IV) and any residual hydrogen peroxide only serves to slow the rate at which nanoceria regains activity via changes in the surface chemistry. The rate of this reversal to cerium (III) is controlled by the standard reduction potential on the surface of the nanoceria in the respective solution. The standard reduction potential for the reaction 1 depends upon the pH of the solution and is found to be below 1.58V above a pH of 1.68 [18].



On the other hand the hydrogen peroxide dissociates via equation 2 and the standard reduction potential (-1.5V) value indicates that it is capable of causing the reverse of equation 1, that is it can oxidize the cerium (present in solution as ions or particles) from (III) to (IV) oxidation state. The addition of excess hydrogen peroxide creates an oxidizing environment during which the ceria is favored in (IV) oxidation state. As the hydrogen peroxide dissociates naturally through equation 2 the shift in reduction potential of the system occurs which then drives the reduction of cerium from (IV) to (III) via equation 1. It must be noted that the hydroperoxy radical (HO_2) is known to play a role in the reversal of oxidation state of nanoceria. Overall the species present in the solution alters the surface potential of the nanoceria and controls the oxidation state as well as chemistry of nanoceria in solution.

Because spectrophotometric determination of cerium (III) levels is difficult in the presence of high concentrations hydrogen peroxide, an alternative method was used for analysis of cerium (III) levels in nanoceria after oxidation by peroxide. An additional sample of nanoceria was treated with 1.0 M hydrogen peroxide to alter surface cerium oxidation state. After 48 hours of hydrogen peroxide treatment 4 units of catalase were added to the oxidized nanoceria. The removal of residual peroxides allows for both determination of SOD mimetic activity in the absence of hydrogen peroxide and further spectrophotometric examination of nanoceria. After the addition of catalase the raw spectral data for nanoceria clearly shows both cerium (III) and cerium (IV) concentrations (Figure 7). If hydrogen peroxide levels were somehow altering SOD mimetic activity of nanoceria, the addition of catalase should cause immediate return of activity. SOD mimetic activity did not return immediately upon removal of hydrogen peroxide by catalase (data not shown) because of the reasons explained in section 3.3. The return of oxidation state and the related SOD mimetic activity will depend upon the surface chemistry which in turn is affected by the environment and surface potentials. The level of cerium (III) did increase concomitantly to the decrease in cerium (IV) levels as assessed by UV-visible spectrum (Figure 7). This further suggests that oxidation state is responsible for the activity of nanoceria and helps to rule out the possibility of artifacts potentially generated by residual hydrogen peroxide.

4.0 Conclusions

Taken together, the results presented in this report give important insight into mechanism behind the SOD mimetic activity of nanoceria and makes a strong case for surface associated cerium (III) sites as the active site for SOD mimetic activity. Among several factors including size/surface area and oxygen vacancy sites, oxidation state appears to play a key role that may be responsible for the effectiveness of nanoceria in catalyzing SOD mimetic activity.

Acknowledgements

We thank Dr. Alex Angerhofer and Witcha Imaram (Department of Chemistry, University of Florida, Gainesville, Florida) for assistance in carrying out EPR studies and data analysis. We would also like to acknowledge Jordan Spence, a Yale University undergraduate (NSF REU nanoscience program) that contributed in the early oxidation studies on this project. This research was supported in part by NSF NIRT (0708172 CBET) to SS as well as NIH R21GM079600-01 to WTS, as well as NSF REU Nanotechnology site grant (EEC 0453436) to SS.

References

1. Hu ZY, Haneklaus S, Sparovek G, Schnug E. Rare earth elements in soils. *Commun Soil Sci Plan* 2006;37(9–10):1381–1420.
2. Medalia A, Byrne B. Spectrophotometric Determination of Cerium (IV). *Anal Chem* 1951;23(3):453–456.
3. Teeguarden JG, Hinderliter PM, Orr G, Thrall BD, Pounds JG. Particokinetics in vitro: dosimetry considerations for in vitro nanoparticle toxicity assessments. *Toxicol Sci* 2007 Feb;95(2):300–312. [PubMed: 17098817]
4. Esch F, Fabris S, Zhou L, Montini T, Africh C, Fornasiero P, et al. Electron localization determines defect formation on ceria substrates. *Science* 2005 Jul 29;309(5735):752–755. [PubMed: 16051791]
5. Campbell CT, Peden CH. Chemistry. Oxygen vacancies and catalysis on ceria surfaces. *Science* 2005 Jul 29;309(5735):713–714. [PubMed: 16051777]
6. Jasinski P, Suzuki T, Anderson HU. Nanocrystalline undoped ceria oxygen sensor. *Sensors and Actuators B-Chemical* 2003 Oct 15;95(1–3):73–77.
7. Korsvik C, Patil S, Seal S, Self WT. Superoxide dismutase mimetic properties exhibited by vacancy engineered ceria nanoparticles. *Chem Commun (Camb)* 2007 Mar;14(10):1056–1058. [PubMed: 17325804]
8. Nikolaou K. Emissions reduction of high and low polluting new technology vehicles equipped with a CeO₂ catalytic system. *Sci Total Environ* 1999 Sep 1;235(1–3):71–76. [PubMed: 10535108]
9. Sayle TX, Parker SC, Sayle DC. Oxidising CO to CO₂ using ceria nanoparticles. *Phys Chem Chem Phys* 2005 Aug 7;7(15):2936–2941. [PubMed: 16189614]
10. Muller FL, Lustgarten MS, Jang Y, Richardson A, Van Remmen H. Trends in oxidative aging theories. *Free Radic Biol Med* 2007 Aug 15;43(4):477–503. [PubMed: 17640558]
11. Niu J, Azfer A, Rogers LM, Wang X, Kolattukudy PE. Cardioprotective effects of cerium oxide nanoparticles in a transgenic murine model of cardiomyopathy. *Cardiovasc Res* 2007 Feb 1;73(3):549–559. [PubMed: 17207782]
12. Schubert D, Dargusch R, Raitano J, Chan SW. Cerium and yttrium oxide nanoparticles are neuroprotective. *Biochem Biophys Res Commun* 2006 Mar 31;342(1):86–91. [PubMed: 16480682]
13. Tarnuzzer RW, Colon J, Patil S, Seal S. Vacancy engineered ceria nanostructures for protection from radiation-induced cellular damage. *Nano Lett* 2005 Dec;5(12):2573–2577. [PubMed: 16351218]
14. Das M, Patil S, Bhargava N, Kang JF, Riedel LM, Seal S, et al. Auto-catalytic ceria nanoparticles offer neuroprotection to adult rat spinal cord neurons. *Biomaterials* 2007 Apr;28(10):1918–1925. [PubMed: 17222903]
15. Borthiry GR, Antholine WE, Kalyanaraman B, Myers JM, Myers CR. Reduction of hexavalent chromium by human cytochrome b5: generation of hydroxyl radical and superoxide. *Free Radic Biol Med* 2007 Mar 15;42(6):738–755. 735–737. [PubMed: 17320757]

16. Frejaville C, Karoui H, Tuccio B, Le Moigne F, Culcasi M, Pietri S, et al. 5-(Diethoxyphosphoryl)-5-methyl-1-pyrroline N-oxide: a new efficient phosphorylated nitron for the in vitro and in vivo spin trapping of oxygen-centered radicals. *J Med Chem* 1995 Jan 20;38(2):258–265. [PubMed: 7830268]
17. Sigler PB, Masters BJ. The Hydrogen Peroxide-induced Ce*(III)-Ce(IV) Exchange System. *J Am Chem Soc* 1957;79(24):6353–6357.
18. Karakoti AS, Kuchibhatla S, Babu KS, Seal S. Direct synthesis of nanoceria in aqueous polyhydroxyl solutions. *Journal of Physical Chemistry C* 2007 Nov;111(46):17232–17240.

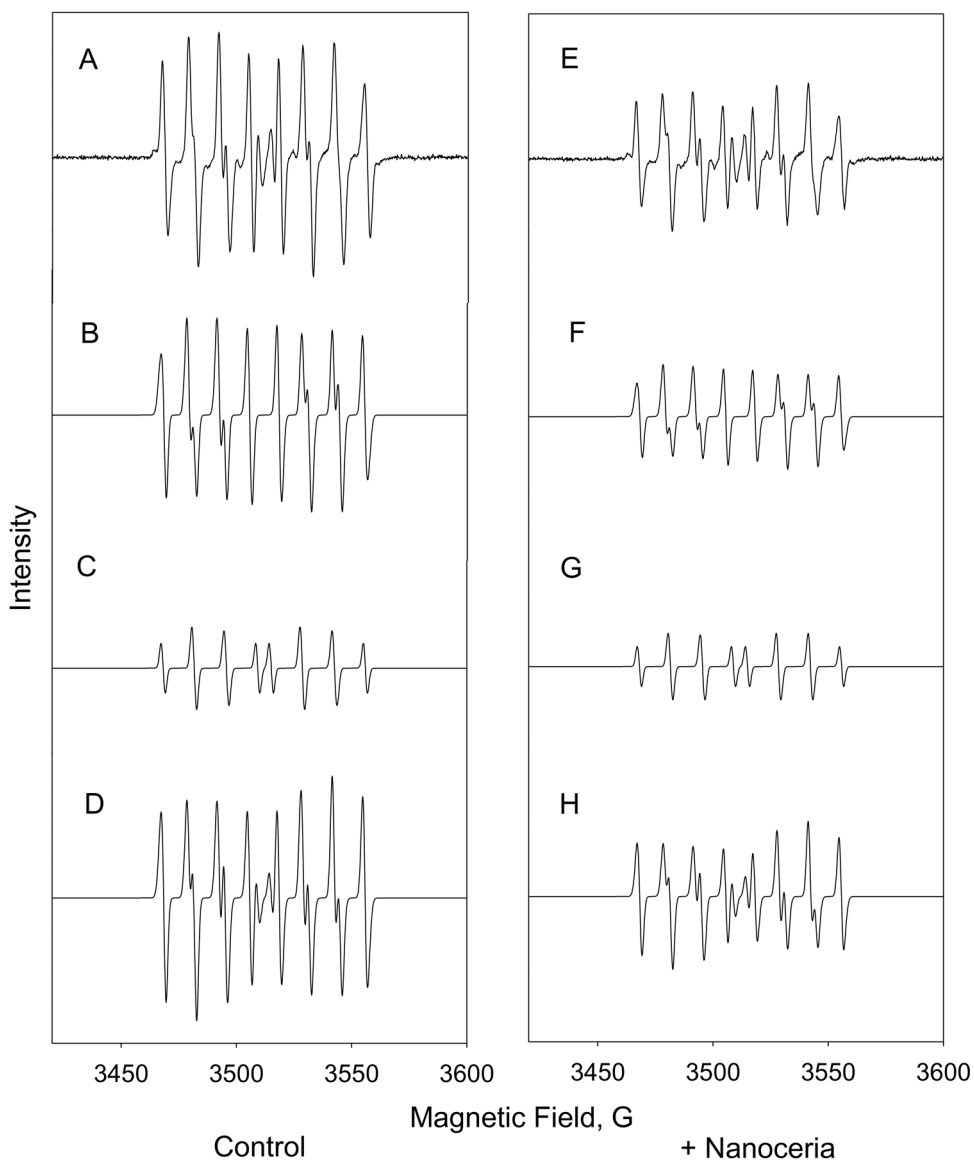


Figure 1. EPR spin-trap analysis confirms SOD mimetic characteristic of nanoceria

The left column represents superoxide DEPMPO adduct signal generated by hypoxanthine and xanthine oxidase in the absence of nanoceria. The right column contains identical conditions with the exception of the addition of nanoceria. (A,E) represent baseline corrected EPR spectrum. (B,F) are simulated signals for superoxide adduct. (C,G) are simulated signals for hydroxyl radical adduct. (D,H) are combined simulated EPR signals.

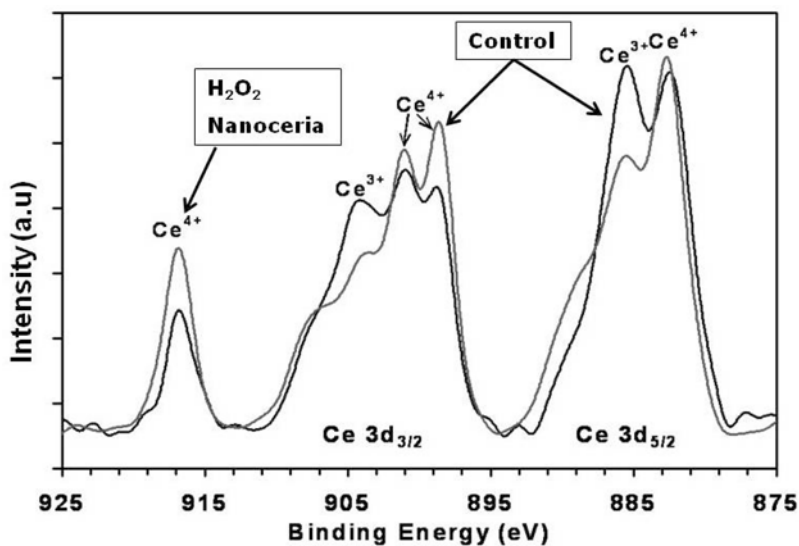


Figure 2. XPS analysis of peroxide treated nanoceria

XPS spectra show the relative concentration of cerium (III) and cerium (IV) oxidation states. The peaks between 875 to 895 eV belong to the Ce 3d_{5/2} while peaks between 895–910 eV correspond to the Ce 3d_{3/2} levels. The peak at 916 eV is a characteristic satellite peak indicating the presence of cerium (IV). The spectra clearly show a difference in the population density of oxidation states of nanoceria upon addition of hydrogen peroxide. After the addition of hydrogen peroxide cerium (III) levels decrease while a corresponding increase in cerium (IV) is observed.

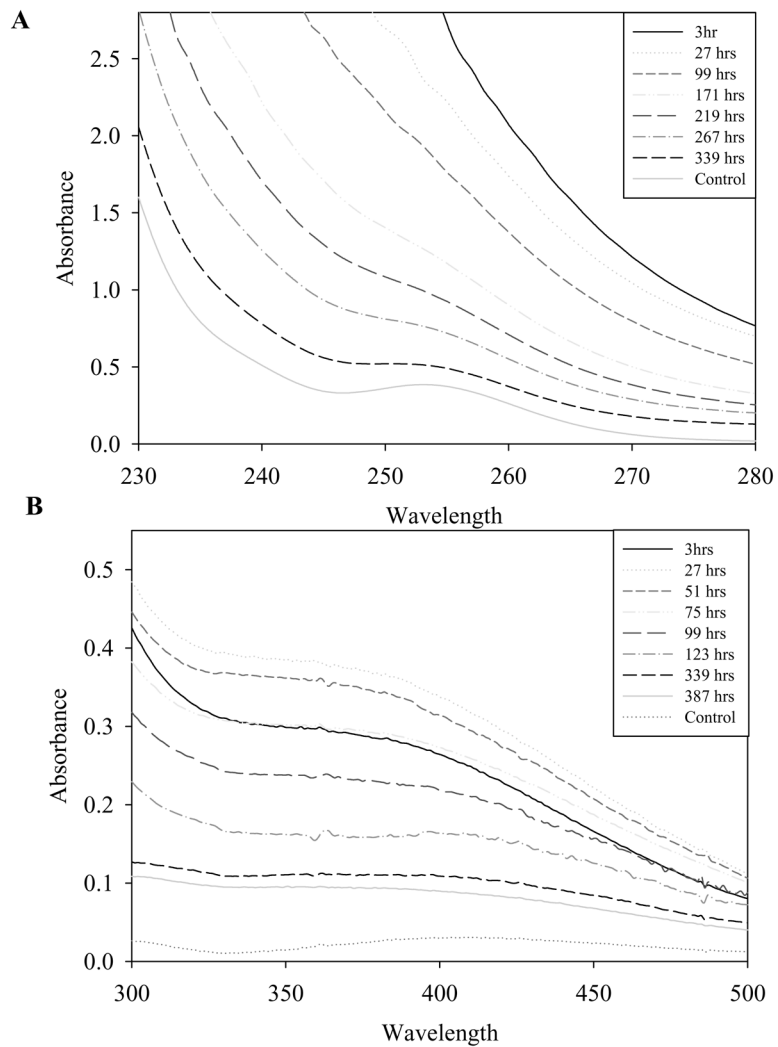


Figure 3. Oxidation of nanoceria leads to reduction in SOD mimetic activity

(A) Competitive inhibition of ferricytochrome C reduction by superoxide after approximately 2 days, Filled circle: control, Open circle: 1.0 M H_2O_2 treated nanoceria, Filled triangle: 100 mM H_2O_2 treated nanoceria, Open triangle untreated nanoceria control. (B) 7 days (C) 9 days (D) 16 days. Control is untreated nanoceria.

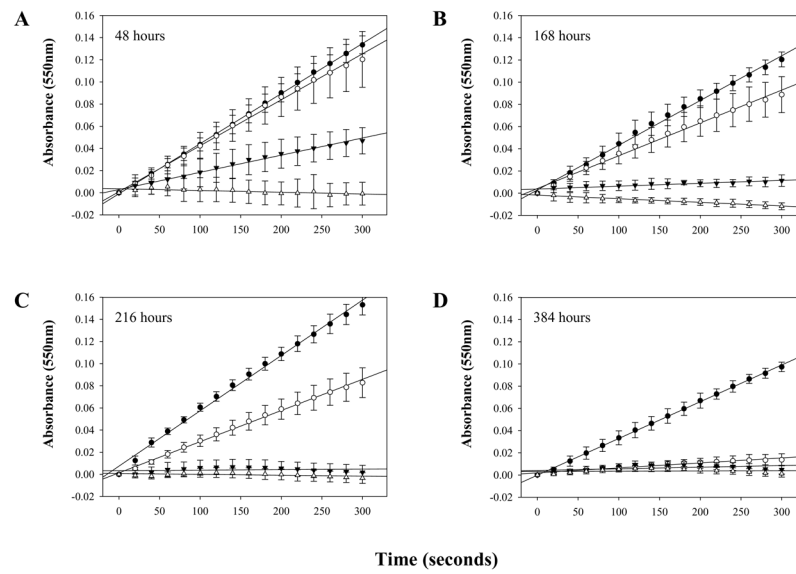


Figure 4. Oxidized nanoceria SOD mimetic activity returns over time

Analysis of nanoceria SOD mimetic activity over time shows a reduction of activity after hydrogen peroxide treatment followed by a slow return in activity over approximately two weeks.

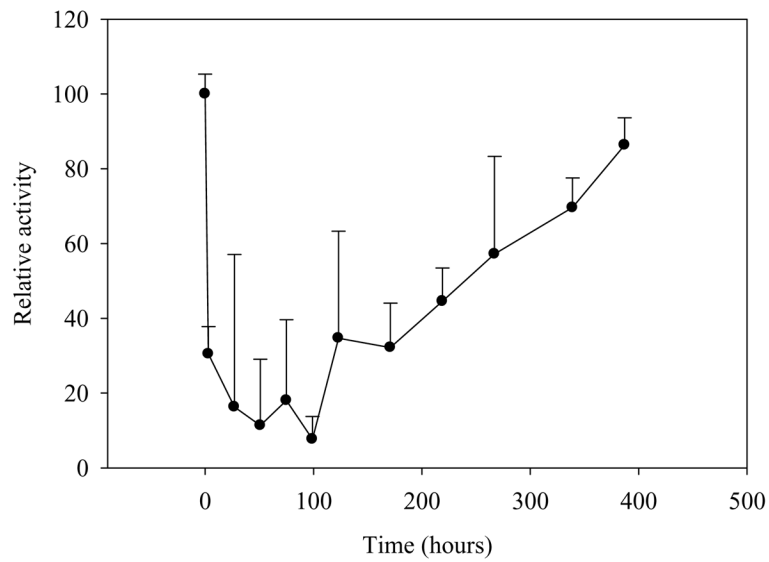


Figure 5. Hydrogen peroxide levels in oxidized samples do not correlate with SOD mimetic activity
Hydrogen peroxide levels were measured using an amplex red assay. Peroxide levels were measured at set time points from 3 hours to approximately 384 hours.

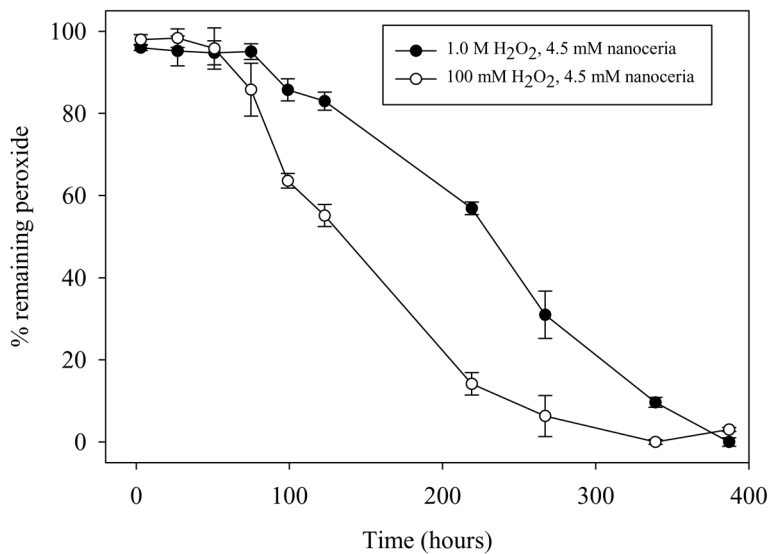


Figure 6. UV-visible spectrophotometric analysis reveal changes in Ce ³⁺/⁴⁺ surface of hydrogen peroxide treated nanoceria

UV-Visible spectra of nanoceria treated with 1.0 M hydrogen peroxide absorbance in the 400 nm range is due to cerium (IV). (A) UV-Visible spectra of nanoceria treated with 1.0 M hydrogen peroxide absorbance peaks at 255 nm are due to cerium (III) absorbance. (B) Spectra of 300 to 400 nm range of hydrogen peroxide treated nanoceria at various time points.

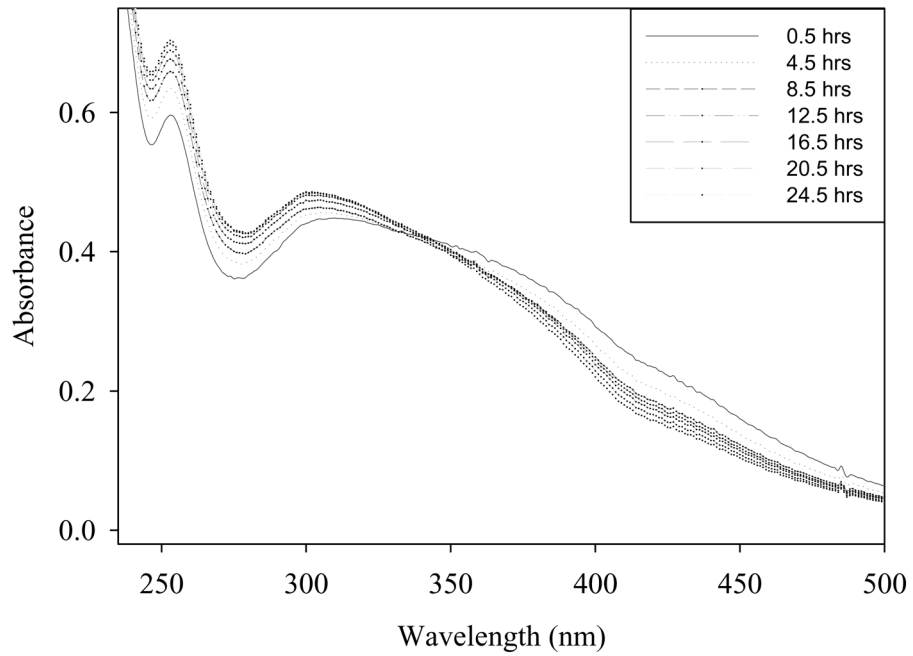


Figure 7. Change in nanoceria spectrum over time after addition of catalase

Spectrophotometric analysis of hydrogen peroxide treated nanoceria. Samples were treated with hydrogen peroxide for two days to insure oxidation of nanoceria then four units of catalase were added to remove excess peroxide. Note the peak at 252 nm corresponding to cerium (III) was previously obscured by excess hydrogen peroxide.